# Cost savings and CO$_2$ emissions reduction potential in the German district heating system with demand response

Yuchen Ju, Joakim Lindholm, Moritz Verbeck, Juha Jokisalo, Risto Kosonen, Philipp Janßen, Yantong Li, Hans Schäfers & Natasa Nord

Published online: 10 Jan 2022.

Submit your article to this journal ↗

Article views: 966

View related articles ↗

View Crossmark data ↗

Taylor & Francis
Taylor & Francis Group

# Cost savings and CO$_2$ emissions reduction potential in the German district heating system with demand response

YUCHEN JU[1,2]* ⓘD, JOAKIM LINDHOLM[1], MORITZ VERBECK[3,4], JUHA JOKISALO[1,2] ⓘD, RISTO KOSONEN[1,2,5] ⓘD, PHILIPP JANßEN[3,4], YANTONG LI[6], HANS SCHÄFERS[3,4] and NATASA NORD[6]

[1]Department of Mechanical Engineering, Aalto University, Espoo, Finland
[2]Smart City Center of Excellence, TalTech, Tallinn, Estonia
[3]Department of Environmental Engineering, Hamburg University of Applied Sciences, Hamburg, Germany
[4]Competence Center for Renewable Energy and Energy Efficiency (CC4E), Hamburg, Germany
[5]College of Urban Construction, Nanjing Tech University, Nanjing, China
[6]Department of Energy and Process Engineering, Norwegian University of Science and Technology, Trondheim, Norway

Demand response (DR) has been an effective technique to maximize the proportion of renewable energies integrated into energy supply systems. This article investigated the benefits of DR on three building types (apartment building, office building and cultural center) and analyzed DR impacts on operation, production costs and CO$_2$ emissions of three district heating (DH) production scenarios. The results indicate that the application of DR cuts 2.8%–4.9% off heating costs for building owners based on different energy production scenarios and building types. From the perspective of DH producers, the large-scale application of DR reduces the total DH demand by 3.6% to 3.9%. It results in higher financial benefits, less CO$_2$ emissions and optimization of energy production in all the analyzed scenarios. The maximum total energy generation cost-saving rate is 12.6%, and the CO$_2$ emissions reduce at most 32.3% because of a more renewable production mix. Moreover, DR control increases the full load operation hours of the heat pump, leading to higher efficiency, and decreases the operation hours of the boilers, leading to less pollution. It indicates that the application of DR effectively decreases fossil fuel usage and improves the energy efficiency of DH systems.

## Introduction

The European Commission has set ambitious targets to cut 40% of greenhouse gas emissions from 1990 levels by 2030 and to realize carbon neutrality by 2050 (European Commission 2018a, 2020). Heating and cooling in buildings and industry take up half of the total EU energy consumption (European Commission 2018b). Moreover, in 2018, fossil fuels were still responsible for 75% of the generation for heating and cooling, while only 19% of energy was

generated from renewable energies (European Commission 2018b). All these figures indicate the immense potential of increasing the share of renewable energies, especially in DH systems, to decrease CO$_2$ emissions.

Werner (2017) stated that there were still high proportions of district heat supply from fossil fuels both in the world (90%) and in the EU (70%) because fossil fuels were the main energy sources for CHP and boilers. The market share of district heating was about 8% and 13% of the total heat demand of buildings in the world and EU in 2014 (Werner 2017). At the EU level, Germany (together with Poland) remains the biggest producer of district heating and cooling (Euroheat & Power and Moczko 2019). Although heat demand is declining because of energy efficiency measures and the retrofitting of old buildings, there is a steady growth in the share of DH within the overall heat market (Euroheat & Power and Moczko 2019). In 2018, CO$_2$ accounted for 88% of all greenhouse gas emissions in Germany, and the ambitious climate target has been set for reducing at least 55% of greenhouse gas emissions by 2030 compared to 1990 levels (BMU (Federal Ministry for the Environment, Nature Conservation and Nuclear Safety) 2020a). However, in 2019 the majority of German buildings were still heated with natural gas and oil, while almost 14% of all heating in German homes was supplied by DH (Freja

2020). Combined heat and power (CHP) plants are the main methods for DH, and CHP plants represented 83% of the total heat generation in 2017. However, the proportion of renewable energies was only 12% of DH consumption (Euroheat & Power and Moczko 2019). Therefore, to realize the carbon neutrality target, increasing the share of renewable energy sources is considered a relevant solution.

In Germany, wind power, photovoltaics and biomass are the most commonly employed renewable sources. In 2019, wind turbines contributed 52% of all renewable electricity, while photovoltaics and biomass each provided approximately 20% of renewable power generation (BMU (Federal Ministry for the Environment, Nature Conservation and Nuclear Safety) 2020a). Although these energies decrease $CO_2$ emissions, the variable generation schedules of wind and solar energy may make energy systems unstable if their proportion increases on a large scale (Robert, Sisodia, and Gopalan 2018). Therefore, to accommodate flexible energy systems, energy consumption on the consumer side also needs to be more flexible. Demand side management has been introduced as a technique to manage the energy demand of buildings and their clusters. Dynamic energy price is employed as one of the incentives for building occupants to actively control their energy demand. These building occupants, once named consumers, have been reclassified as prosumers, who have or desire to have a more active role in energy markets (Miller and Senadeera 2017; Zafar et al. 2018). Therefore, the energy demand of buildings and their clusters could be optimized, and costs for purchasing electricity and heating energies are reduced through DR control (Gelazanskas and Gamage 2014; Shan et al. 2016). These buildings are energy-flexible according to user needs, local climate conditions and grid requirements (Jensen et al. 2017).

Various techniques have been proposed to improve the energy flexibility of buildings and their clusters or increase monetary benefits based on dynamic electricity or DH prices. Massive building structures are operated as thermal energy storage (TES) in the DR control. When energy prices are low, the indoor air temperature could be increased, and heat is charged in the structures. This part of the heat is discharged to maintain the indoor air temperature at an acceptable level when energy prices are high. Therefore, residential buildings with different levels of thermal insulation were modeled and the impacts of charging and discharging heat were evaluated (Le Dréau and Heiselberg 2016; Johra, Heiselberg, and Le Dréau 2019). Furthermore, three flexibility factors have been defined to quantify the characteristics of building thermal mass by the DR control for residential buildings: available storage capacity, storage efficiency and power shifting capability (Reynders, Diriken, and Saelens 2017). Available storage capacity represents the amount of energy that can be stored in thermal mass during limited charging hours. Storage efficiency describes the percentage of stored energy that can be successfully discharged to maintain a comfortable indoor air temperature. Power shifting capability was defined as a measure for the instantaneous energy flexibility, which describes the relationship between the change in heating power and the duration of maintaining this shift. A cluster of detached houses (159 buildings) in Denmark was simulated to exploit the thermal inertia benefits with the

DR control for a community (Hedegaard et al. 2019). In the study, a price-based DR control combined with thermal storage decreased the DH demand of domestic hot water (DHW) power peaks by 5%.

The cost-saving potential from DR control at the building level has been investigated to encourage prosumers to actively control their energy demand. The cost-saving potential of dynamic electricity prices has been fully analyzed in various studies (De Coninck and Helsen 2016; Hu and Xiao 2018; Junker et al. 2018) and some of them also investigated the potential of $CO_2$ emissions reductions (Song et al. 2014; Knudsen and Petersen 2016). Moreover, for district heated buildings, a study of a Finnish office building showed that DR control with predictive control algorithms decreased annual heating energy costs by a maximum of 5% (Wu et al. 2021). The real-time pricing-based DR of space heating and ventilation applied in an office building in Finland decreased heating energy consumption by 3% and heating energy costs by 6% (Vand et al. 2020). In addition, a DR control algorithm that prioritized DHW usage has been presented and nearly 15% of power peaks were decreased in student dormitories. In the heating period of February and March, there was a 9% annual cut in energy, costs and greenhouse gas emissions (Ala-Kotila, Vainio, and Heinonen 2020).

Besides the building-level analysis, more scholars began to investigate DR benefits with regard to energy systems. The optimization of energy supply units with renewable energies has been analyzed (Tereshchenko and Nord 2016). Moreover, a short-term TES, such as a water tank, has been integrated to effectively decrease the demand for peak power and make system operation more flexible. To quantify the flexible operation, temporal flexibility, power flexibility and energy flexibility have been classified and mainly adopted in the analysis of CHP systems (Stinner, Huchtemann, and Müller 2016). These factors are defined to describe charging or discharging hours, the amount of charging and discharging powers or energies of TES (Nuytten et al. 2013). In addition, researchers investigated the cost savings potential of DR. Simulation results from a Finnish DH network concluded that through the implementation of hot water thermal storage, DR control saved 1.4% of heat production costs, while $CO_2$ emissions were reduced by only 0.8% at most (Salo et al. 2019). The DR control applied in a heat pump system with a hot water storage tank provided an energy cost saving of 5% in Denmark (Knudsen and Petersen 2017). Moreover, by introducing a realistic demand side management mechanism in a Danish DH network, it was estimated to decrease energy costs by 11% (Cai et al. 2018).

Although DR effects on buildings or their clusters and energy systems have comprehensively addressed cost, time, power and energy aspects, DR effects are examined separately. There are few studies where DR effects have been analyzed simultaneously and together on buildings and their DH systems. Kontu et al. (2018) analyzed ways in which different DR control strategies affected DH systems of three sizes. Hourly heat power data with different building types were measured to establish the consumption profiles of the
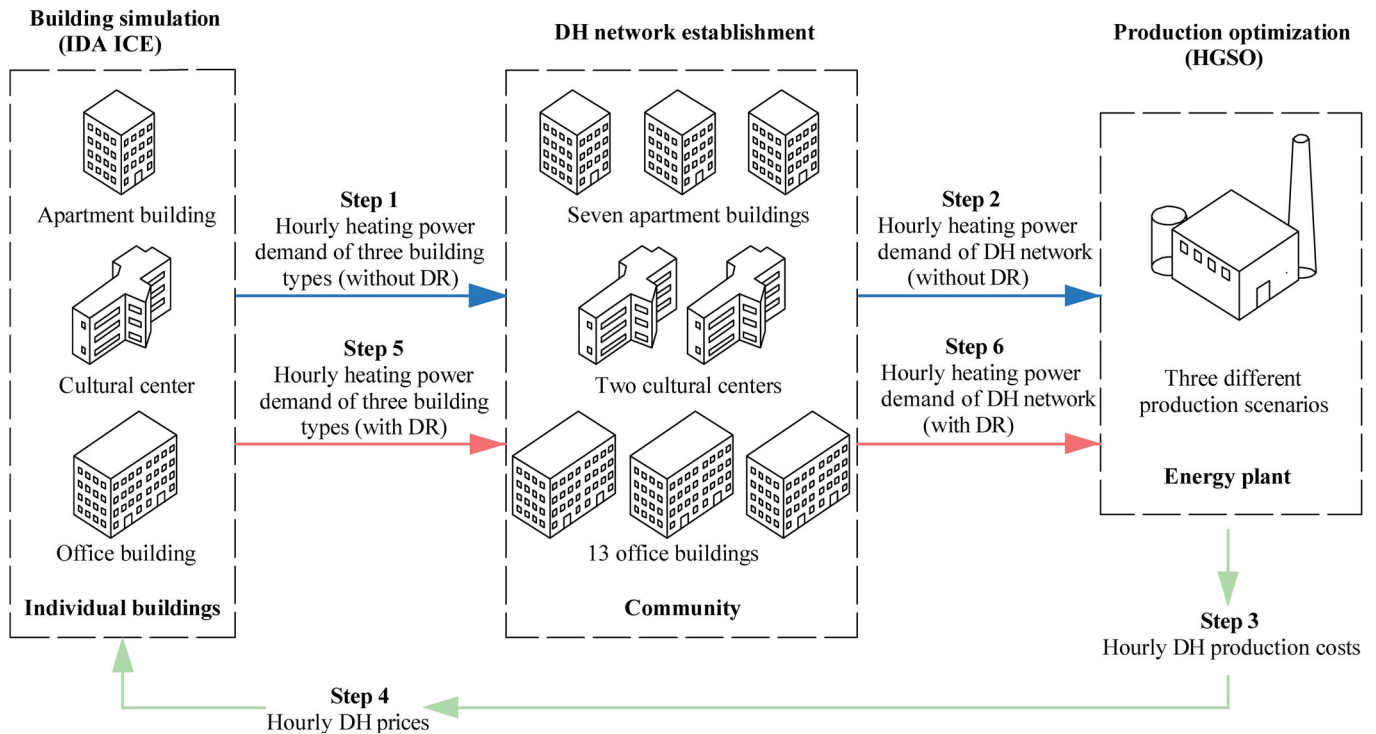
**Fig. 1.** Description of the whole simulation process.

DH systems so that the control strategies were designed to optimize the operation of the DH systems without the building level being linked to the analysis performed. Moreover, the study did not conclude the results of $CO_2$ emissions reductions of the DH systems. Dominković et al. (2018) analyzed the DR benefits of DH production costs. They also discussed the impact of thermal mass storage in buildings on DH production. The article focused on production cost savings while the results did not involve energy cost savings at the building level. In addition, the article did not evaluate the effect of DR on the operation time of production units.

The novelty of this study is that the DR control impacts on buildings and DH production were analyzed in tandem and considered the interaction between them. According to the authors' best knowledge, this is the first paper to investigate the effects of DR on indoor temperature conditions, cost savings for building owners, and from a producer's point of view, $CO_2$ emissions and operation time of DH production units together. The interaction between buildings and energy production was considered in the modeling in German conditions. The building-level DR control was designed based on hourly DH prices generated by employing different production mixes. In return, the building-level DR control changed the power demand of the whole established DH network and further affected DH production.

This article aims to examine DR benefits for both building owners and energy producers. Firstly, the building-level DR control was applied in three building types (apartment building, cultural center and office building). Then, a DH network for a community of 22 buildings representing these three building types was established for the production-level simulation. There were three production scenarios with

different heat generation mixes. Finally, the DR impacts on indoor temperature conditions, cost savings for building owners and the producer, DH production operation and $CO_2$ emissions were investigated under three different production scenarios.

## Methodology

This chapter is divided into three sections. The first section introduces the whole simulation process. The second section focuses on the description of the building-level simulation, including simulation process, tool, weather data and simulated buildings. Finally, the last section mainly presents the simulation process, tool and scenarios at the production level.

### Description of simulation process

Figure 1 describes the whole simulation process, which is called as a "co-simulation" in this article referring the use of two simulation tools and their combination. Firstly, three building types, apartment building (AB), cultural center (CC) and office building (OB), were simulated without DR using the dynamic building simulation tool IDA ICE. Secondly, a DH network consisting of these three building types was established with a similar annual heat demand to an actual DH network in Hamburg. It was assumed that each building cluster consisted of a single building type. Therefore, the hourly power demand of the network was aggregated by the hourly power demand data of the three clusters. Thirdly, the DH network demand data were used as
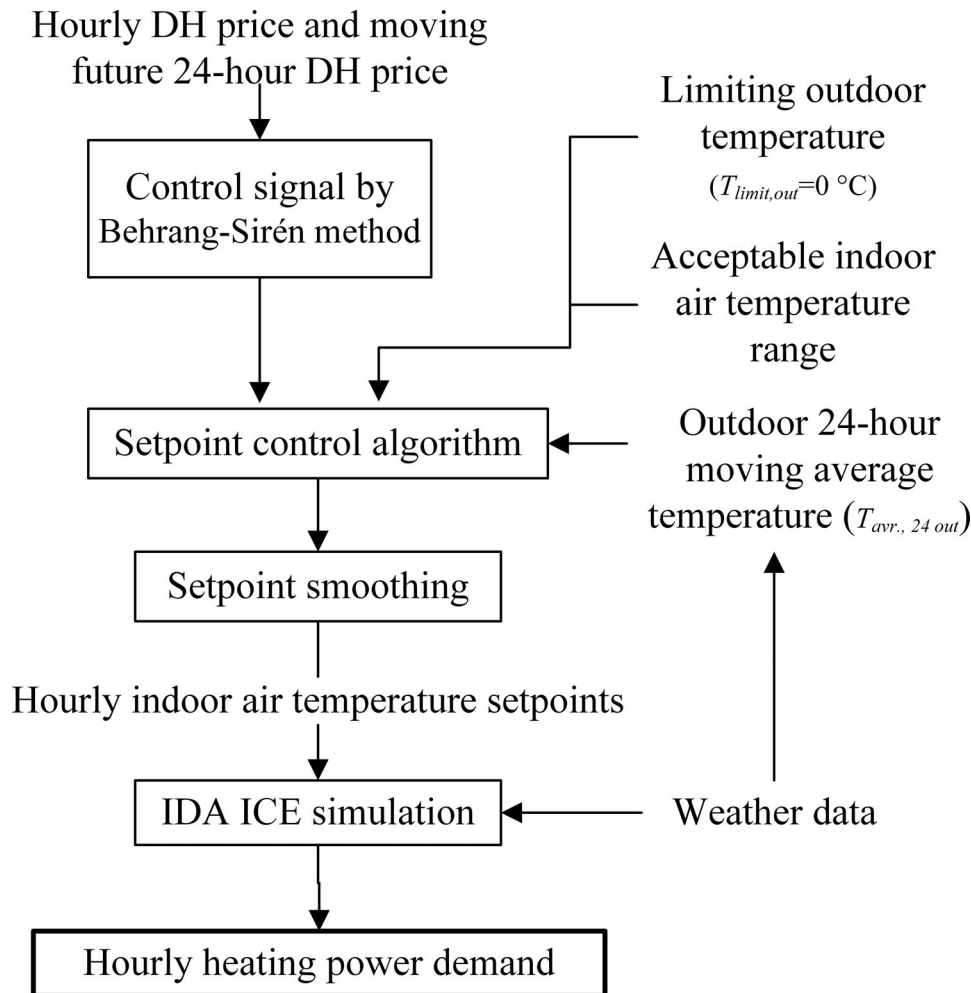
**Fig. 2.** Flow chart of building-level simulation process with DR control.

an input to a production simulation tool HGSO and three production scenarios were employed in the established DH network for comparison. The total production costs and $CO_2$ emissions of the DH network without DR were calculated using a dynamic production optimization tool HGSO (Tillmann 2017). DH prices for consumers were also calculated by HGSO according to hourly production costs of different scenarios without DR. After that, three building types were simulated based on these DH prices by rule-based DR control, and the procedure for calculating the total production costs and $CO_2$ emissions with DR was repeated as mentioned above, respectively.

### Building-level simulation

*Building-level simulation process*
Figure 2 describes the building-level simulation process of a rule-based DR control. It has predefined and fixed rules considering different triggers to realize DR control. In this study, according to the dynamic DH price trigger, the indoor air temperature was changed for load shifting from high to low price periods. It was employed because of its simplicity, easy implementation and low computational power demand. The

Behrang-Sirén method (Alimohammadisagvand, Jokisalo, and Sirén 2018; Vand et al. 2020) was applied to change hourly DH prices and the moving future 24-hour prices into control signals. The moving future 24-hour price is the DH price for the subsequent 24 hours. The outdoor 24-hour moving average temperature, acceptable indoor air temperature range and limiting outdoor temperature were considered in the setpoint control algorithm. The outdoor 24-hour moving average temperature is the average outdoor temperature of the past 24 hours. The minimum indoor air temperature setpoint (20 °C) was defined based on the thermal environmental category II of standard SFS-EN 16798-1 (2019). The maximum acceptable indoor temperature setpoint (23 °C) was set similar to Suhonen et al. (2020). The setpoint smoothing technique was employed to prevent the power load from increasing sharply (Suhonen et al. 2020; Ju et al. 2021). Finally, the final hourly indoor temperature setpoints were obtained for three building types.

*Building simulation tool and weather data*
This study chose the building simulation tool IDA Indoor Climate and Energy (IDA ICE) version 4.8 for simulation (Sahlin 1996). IDA ICE is a dynamic multi-zone simulation software package. It allows users to model the characteristics
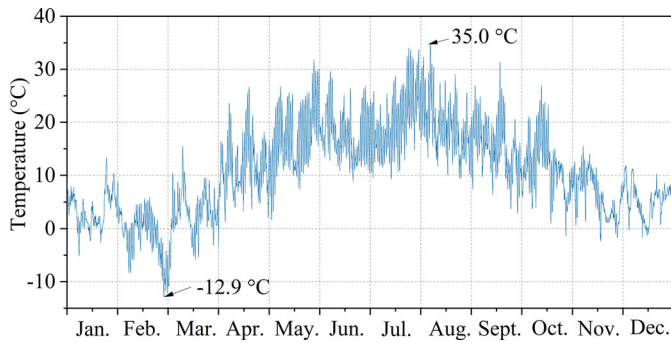
**Fig. 3.** Hamburg outdoor temperature for 2018.

of a building and its technical systems such as building geometry and structures, HVAC systems and user profiles. It has been validated against the EN 15255-2007 and EN 15265-2007 standards (Equa Simulation 2010a). In addition, this software has been validated in several studies (Bring, Sahlin and Vuolle 1999; Equa Simulation 2010b; Moosberger 2007). This provides a strong justification for IDA ICE simulation in this article.

Buildings were simulated with the measured weather data for Hamburg from 2018. Figure 3 presents the annual outdoor temperature with the maximum and minimum temperatures of 35 °C and −12.9 °C, respectively. The heating degree days at the indoor air temperature of 15.5 °C are 2147 °C·d and annual average temperature is 10.8 °C (Kozarcanin, Andresen, and Staffell 2019; European Environment Agency 2021).

*Description of simulated buildings*
Table 1 shows the parameters of the three building types. The apartment building was initially built during the 1930s. The cultural center and office building were built in the early 1980s, but have been recently renovated. Internal heat gains of occupants were chosen based on an activity level of 1.2 MET with a clothing of $0.75 \pm 0.25$ clo, which indicates sedentary activity and normal clothing (CEN (The European Committee for Standardization) 2007). The heating energy demand for DHW of three building types was set at 17, 4 and 6 kWh/$m^2$, respectively (Loga and Imkeller-Benjes 1997). In Table 1, design heating power was defined as the heating power demand of water radiators and ventilation in each building type at the design outdoor temperature of −12 °C. Ventilation systems are described in Table 2. The design heating power of ventilation for each building type was calculated based on the air change rate listed in Table 2. The value is zero in the apartment building because of natural ventilation. Table 1 also shows that water radiators are the primary heating devices in the cultural center providing 61% of the heating power. On the other hand, the ventilation system in the office building contributes 64% of the heating power supply.

The DH substation efficiency was assumed to be 0.97 (Suhonen et al. 2020). The control curves of the inlet water temperature of water radiators with different outdoor temperatures are shown in Figure 4. The maximum inlet water temperature was 80 °C in the apartment building, while it was

70 °C in the cultural center and office building. The design temperatures of radiators were set to 80/60 °C for apartment buildings and 70/40 °C for other building types. These values were selected according to the ages of these German buildings. There were no mechanical cooling systems in these buildings. In addition, radiators in the simulated buildings were equipped with electronic radiator valves (motor-operated valves) that are able to control the room air temperature accurately.

Table 2 provides details about the ventilation systems for the three building types. There was natural ventilation in the apartment building and mechanical ventilation in the other building types. In general, the mechanical ventilation systems were turned on two hours before the occupancy hour started and turned off one hour after closing the cultural center and two hours after closing the office building. The air change rate of the naturally ventilated apartment building was set based on Mikola, Kalamees, and Kõiv (2017). Design airflow rates for the mechanically ventilated spaces were selected by REHVA's health-based ventilation guidelines for Europe (Seppänen et al. 2012). Pressure losses of the ventilation duct system and efficiencies of fans were chosen based on the EN 13779 (CEN (The European Committee for Standardization) 2007) standard.

### Production-level simulation

*Production-level simulation process*
The production-level simulation intents to achieve comparable results of DR impacts on DH operation, costs and $CO_2$ emissions with different scenarios. Therefore, a sequence of calculations and simulations were performed, and the procedure of the production-level simulation has been depicted in Figure 1. The hourly heat demand of three example buildings without DR for the whole year was calculated for the first step. The purpose is to establish a DH network with a close annual heat demand as an actual DH network in Hamburg. The average yearly heat demand for 2017 and 2018 from all substations of a local DH system was adopted for this study. The actual community consists of an existing building stock with 22 apartment buildings (yearly heat demand of 3444 MWh), five office buildings (yearly heat demand of 3735 MWh) and two cultural centers (yearly heat demand of 721 MWh). Therefore, the established community includes seven apartment buildings, 13 office buildings and two cultural centers according to the simulated yearly heat demand without DR of each building type. The deviation of the actual average yearly heat demand and that of the established DH network is 0.19%. Consequently, the total production costs and $CO_2$ emissions for the established DH network and DH prices without DR were calculated using the dynamic optimization tool HGSO with three different production scenarios. The tool, heat generation schedule optimizer (HGSO), can optimize and output the most economical heat generation schedule of production units under technical and economic limitations (Tillmann 2017).

In this article, the calculation of DH prices was performed in three steps, as shown in Figure 1: (1) The input

**Table 1.** Building model parameters.

| Parameters | | Apartment building | Cultural center | Office building |
|---|---|---|---|---|
| Heated net floor area (m$^2$) | | 4885 | 3937 | 2383 |
| Number of floors | | 4 | 3 | 4 |
| Envelope area (m$^2$) | | 4780 | 6921 | 3855 |
| Window/envelope area | | 7.6% | 8.8% | 9.5% |
| U-value (W/m$^2$·K) | External walls | 1.7 | 0.2 | 0.2 |
| | Roof | 1.4 | 0.19 | 0.19 |
| | Ground slab | 1.0 | 0.28 | 0.28 |
| | Windows | 3.0 | 3.0 | 3.0 |
| Air leakage rate, $n_{50}$ (1/h) | | 7.0 | 3.0 | 4.5 |
| Usage time | | Continuous | 8 am–9 pm (every day) | 8 am–4 pm (working days) |
| Annual internal heat gains of equipment (kWh/m$^2$·a) | | 11 | 9 | 2 |
| Annual internal heat gains of lighting (kWh/m$^2$·a) | | 16 | 17 | 11 |
| Heating power of radiators at design temperature (kW) | | 225 | 175 | 101 |
| Specific heating power of radiators at design temperature (W/m$^2$) | | 46 (100%[A]) | 44 (61%[A]) | 42 (36%[A]) |
| Heating power of ventilation at design temperature (kW) | | 0 | 111 | 178 |
| Specific heating power of ventilation at design temperature (W/m$^2$) | | 0 (0%[B]) | 28 (39%[B]) | 75 (64%[B]) |
| Total specific heating power at design temperature (W/m$^2$) | | 46 | 72 | 117 |

[A] Ratio of the design heating power of water radiators and the total design heating power in each building type.
[B] Ratio of the design heating power of ventilation and the total design heating power in each building type.

**Table 2.** Ventilation systems for simulated buildings.

| Building type | Ventilation system | Air change rate | Operation time |
|---|---|---|---|
| Apartment building | Natural ventilation | 0.24 1/h | Always on |
| Cultural center | Mechanical supply and exhaust ventilation (CAV) without heat recovery for kitchen, restaurant, basement and hall | 1.7–2.36 l/s, m$^2$ | 8 am–10 pm 7 am–10 pm (Basement) |
| | Mechanical exhaust ventilation (CAV) for toilets | 2.5–4.5 l/s, m$^2$ | Always on |
| | Natural ventilation for other spaces | 0.2–0.43 l/s, m$^2$ | Always on |
| Office building | Mechanical supply and exhaust ventilation (CAV) without heat recovery | 2.1 l/s, m$^2$ | 6 am–6 pm for workdays |

data (hourly heating power demand of DH network without DR) was processed. (2) The dynamic optimization tool HGSO calculated the hourly heat production costs with different production scenarios. (3) These hourly heat production costs were normalized to fit the real DH price of 91.2 €/MWh of the actual DH network in Hamburg provided by Vattenfall Wärme and Hamburg GmbH (2019). These prices were calculated based on operational expenditure. Therefore, capital expenditure was not taken into consideration.

*Simulation tool*
The optimization tool HGSO was enhanced based on the study by Tillmann (2017). Its objective is to find the most economical heat generation schedule of a modeled plant portfolio by considering technical and economic constraints. The model is defined as a mixed-integer linear programming problem (MILP), which was applied for schedule generation of energy

plants (Christidis 2019; Bagherian et al. 2021). For solving the optimization problem, the tool adopts the open-source solver "CBC" (Forrest and Lougee-Heimer 2005). Alternative optimization approaches in DH networks were summarized in Sameti and Haghighat's (2017) research.

The HGSO results were validated with reference data using the commercial optimization tool BoFiT. BoFiT is a standard optimization platform for smart grid energy and operation delivered by ProCom GmbH (Lu and Shumei 2018; Vogt, Marten, and Braun 2018; ProCom GmbH 2020a). BoFiT also maps the given plant portfolio into a MILP model, which is widely used in DH heating grid optimization (Merkert, Haime, and Hohmann 2019; Merkert and Castro 2020). It has been validated in several studies (Henriksson and Rudén 2018; ProCom GmbH 2020b). To validate the tool, results of both optimizers with the same input data were compared with the focus on the total costs
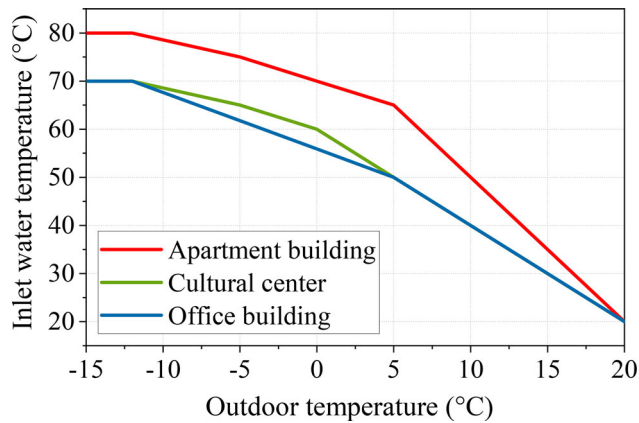
**Fig. 4.** Inlet water temperature control curves as a function of outdoor temperature.

of heat generation. Table 3 lists the optimization results of these two tools with the local DH system consisting of a CHP and boilers. The difference in the total costs is 0.4%.

Table 3 shows, besides the costs, the results concerning the total generated heat of both CHP and boilers and the full load operating hours of the CHP for both tools. The deviations occur because, contrary to HGSO, which investigates the economic daily optimum and has a fixed storage limit charge of 50% at midnight, BoFiT analyzes the whole year and has no restrictions on storage. This difference is negligible for the purposes of this study. Figure 5 depicts the variance between the optimized heat generation for the CHP within a selected period. Overall, the operational schedules are quite similar, and the peak heat loads in each operational period are close. All these results provide a strong justification for the use of HGSO in this article.

*Production scenarios*
Table 4 lists production combinations in three production scenarios. Scenario 1 corresponds to the actual mix of generation units of the Hamburg DH system. DH prices are affected by production combinations. The considered unit types are CHP, boilers, heat pumps, electric heaters and solar thermal collectors. The main purpose of the unit type selection was to have one scenario with a mixture of electricity feed-in and electricity consumption, and electricity consumption only. Furthermore, the DR control algorithm reacts according to price variations. More fluctuated prices have a more obvious impact on DR control signals. Therefore, various unit combinations were calculated by HGSO and compared with regard to the fluctuation and alteration of the hourly production costs. The HGSO tool only considered generated heat and heat demand and neglected supply water temperature levels. It was considered that all chosen generation units were capable of providing the required temperature, since the local district heating network was of the third-generation and operated below 100 °C (Revesz et al. 2020). Furthermore, the effects of varying heat pump COP values on the supply temperature were neglected and we decided not to create different heat pump scenarios for discussion on the impact of COP values on demand response. Based on these specifications and the preference for renewables and sector coupling, two production scenarios, namely scenario 2 and

scenario 3, were selected for comparison as shown in Table 4. It is possible to reach the required supply temperature level with the generation unit types of scenarios, 2 and 3.

For units in the scenario 1, the maximum powers were taken from the actual production units based on the local DH system. The CHP unit can generate up to 0.737 and 0.527 MW of heat and electricity power. The CHP unit and gas boilers 1 and 2 are also components of scenario 2. Therefore, these units have the same maximum powers as those in scenario 1. For the heat pump, the electric heater and the solar thermal unit, their maximum powers were set to cover the maximum heat demand. The energy source of the heat pump was not specified because it was not relevant for the optimization. The COP of the heat pump was 4 in all conditions. The generated energy of the solar thermal supplied the load directly. In scenario 2, gas boiler 3 was replaced by a heat pump with a slightly higher capacity according to heat pump models on the market, and the solar thermal collectors were added to increase the renewable energy generation. In scenario 3, the maximum power of the heat pump was limited by the largest available capacity currently on the market, which can generate about 2 MW of heat with 0.5 MW electricity consumption. The maximum electricity power for the electric heater unit to generate heat is 3.74 MW. The maximum power of the solar thermal unit was set based on a measured time series of the hourly generated solar heat by the local solar thermal supply unit.

For every hour, the heat demand had to be covered by a combination of units and a heat store. There was a hot water tank integrated in each scenario with a heat capacity of 1.4 MWh. All the units were able to charge the water tank. It could be operated temporarily to balance over- or under-production. The storage tank must be filled to 50% by the generation units in all scenarios at the end of the considered period (24 hours). Depending on the price of electricity on the electricity market, HGSO optimized the most economical way to generate the demanded heat. It resulted in an hourly schedule of the unit and storage operations. When the electricity price was high, the heat generated from CHP units was maximized to cover the heat demand and the extra generated electricity was sold for high profits. Since the CHP units are fed with bio-methane, profits increase due to the granted governmental subsidy. In scenario 1, the CHP unit was operated firstly most of the time because of higher earnings. Boilers would be activated when the power of the CHP was insufficient to cover the heat demand. However, when the market electricity price was very low or negative, boilers might be operated initially to cover the demand according to a lower cost of production compared with the CHP unit.

Figure 6 depicts the operation schedule of the units and the heat storage system of scenario 2. Market electricity price, limitations (minimum runtime/downtime of production units and minimum generation) and the threshold value (depending on the current electricity price and the average price of the previous month) were considered for optimization. In scenario 2, depending on the market electricity price, electricity generated by CHP units could be consumed by the heat pump. Firstly, heat demand was covered by the

**Table 3.** Comparison of BoFiT and HGSO production optimization tools for an example year.

| Tools | Total costs (%) | Generated heat CHP (MWh) | Generated heat Boilers (MWh) | Full load hours (h) |
|---|---|---|---|---|
| BoFiT | 100% | 5069 | 1446 | 6924 |
| HGSO | 99.6% | 5039 | 1496 | 6154 |
| Difference | 0.4% | −30 | 50 | −770 |
| | | −0.6% | 3.3% | −11.1% |
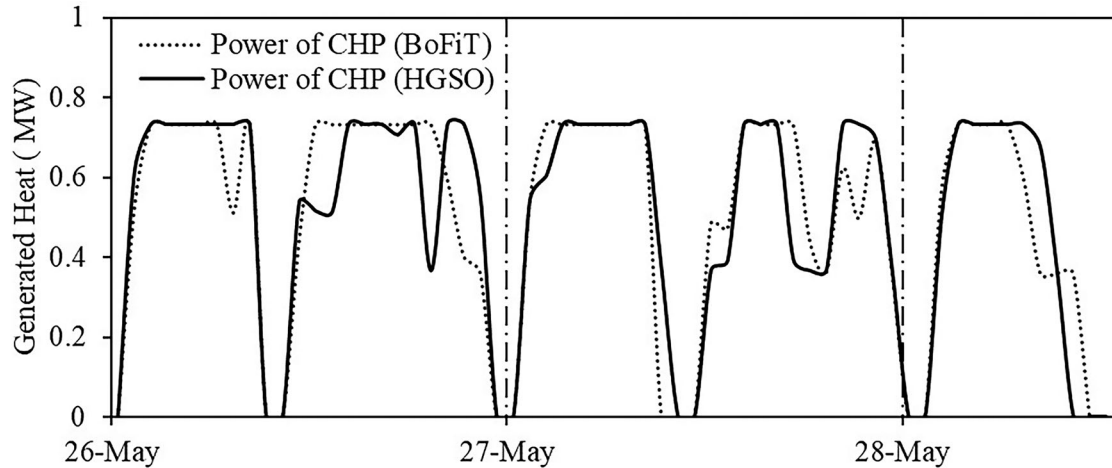


**Fig. 5.** Optimized heat generation of CHP for an exemplary period.

**Table 4.** Heat generation units and their maximum powers in different scenarios.

| Generation unit | Scenario 1 Heat/electricity power (MW) | Scenario 2 Heat/electricity power (MW) | Scenario 3 Heat/electricity power (MW) |
|---|---|---|---|
| CHP | +0.737 / +0.527 | +0.737 / +0.527 | − |
| Gas boiler 1 | +1.950 / 0 | +1.950 / 0 | − |
| Gas boiler 2 | +1.100 / 0 | +1.100 / 0 | − |
| Gas boiler 3 | +1.100 / 0 | − | − |
| Heat pump (HP) | − | +1.320 / −0.330 | +2.000 / −0.500 |
| Electric heater (EH) | − | − | +3.550 / −3.740 |
| Solar thermal (ST) | − | +0.483 / 0 | +0.483 / 0 |
| Total heat power | 4.887 | 5.590 | 6.033 |

solar thermal and heat storage (1.4 MWh) units. After that, the operation order of the CHP and heat pump depended mainly on production costs. If the profit from heat pump production was higher than that of the CHP unit, the heat pump would generate initially to cover the remaining heat demand. Otherwise the CHP unit would be operated first. The boilers were never generated to cover heat demand if the heat pump or CHP could cover it in this step. The reason is that either the CHP or the heat pump generates heat with lower costs. Then, in the following step, if CHP had been chosen in the latter step and it could not cover all the demand, the heat pump would cover the additional demand when the market electricity price was low. When the market electricity price was high, the boiler would cover the additional heat demand.

In scenario 3, when the market electricity price was greater than zero, the remaining heat, which could not be covered

with solar thermal and the hot water tank, was provided by the heat pump or this part of the heat was covered by the electric heater unit when the market electricity price was negative.

*Community-level scaling of DR savings*

The scaling technique was applied in this study after step 6, as shown in Figure 1. The intention is to divide the total saved costs of each scenario by DR into energy reduction savings and DR savings. Energy reduction savings are caused by the decrease in indoor air temperature. DR savings are caused by shifting heating power from high production cost periods to low production cost periods. Each scenario without DR was scaled based on annual total heating energy with DR. After that, the tool HGSO optimized these scaled scenarios for production costs. Therefore, compared with each scaled scenario, these saved production costs with DR are only DR savings. The hourly heat power of each scenario without DR was scaled to reach the yearly total heating
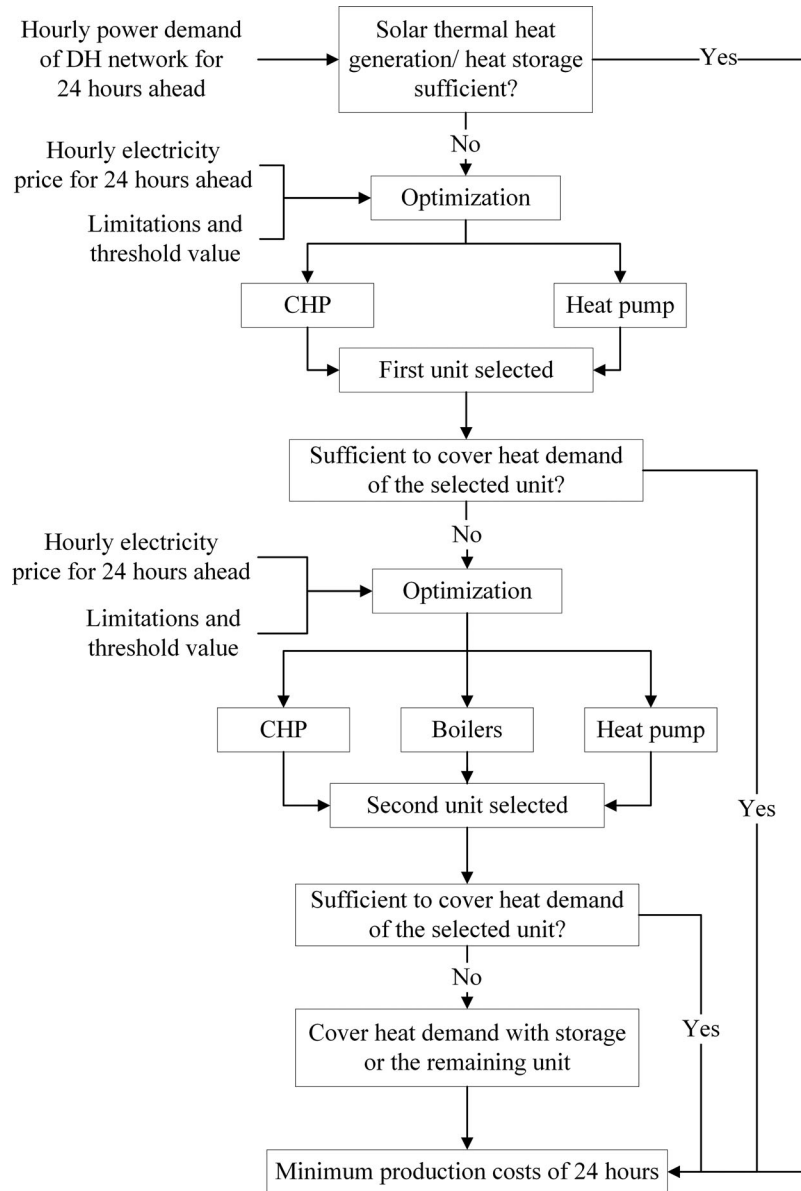
**Fig. 6.** Operation schedule of units and the heat storage system of scenario 2.

energy with DR as shown in Eq. (1):

$$Q_{scaled}(t) = Q_{without\ DR}(t) \frac{\sum_{t=1}^{8760} Q_{with\ DR}(t)}{\sum_{t=1}^{8760} Q_{without\ DR}(t)} \qquad (1)$$

where $t$ is the time slot with the range from 1 to 8760, h; $Q_{scaled}(t)$ is the scaled hourly heat demand of the DH network, MWh; $Q_{without\ DR}(t)$ is the hourly heat demand of the DH network without DR, MWh; and $Q_{with\ DR}(t)$ is the hourly heat demand of the DH network with DR, MWh.

### Description of studied building cases

Figure 7 introduces the studied building cases. Firstly, each building was simulated without DR and then the annual DH energy costs were calculated based on three DH prices, respectively. After that, three buildings were simulated with DR according to three DH prices. For example, apartment building cases with or without DR in scenario 1 were named *AB with DR Scen1* and *AB without DR Scen1*. Therefore, there are 18 studied cases in total.

## Demand response in district heating system

### DH prices for different production scenarios

Production costs in this study were defined as shown in Eq. (2):

$$C_{prod.} = C_{exp.} - C_{rev.} \qquad (2)$$

where $C_{prod.}$ is production costs, €; $C_{exp.}$ is total expenses for fuel (CHP and boilers) and electricity (heat pump and electric heater units), €; and $C_{rev.}$ is the revenue from selling electricity by CHP unit (including government grants), €. The total expenses for fuel were calculated as:
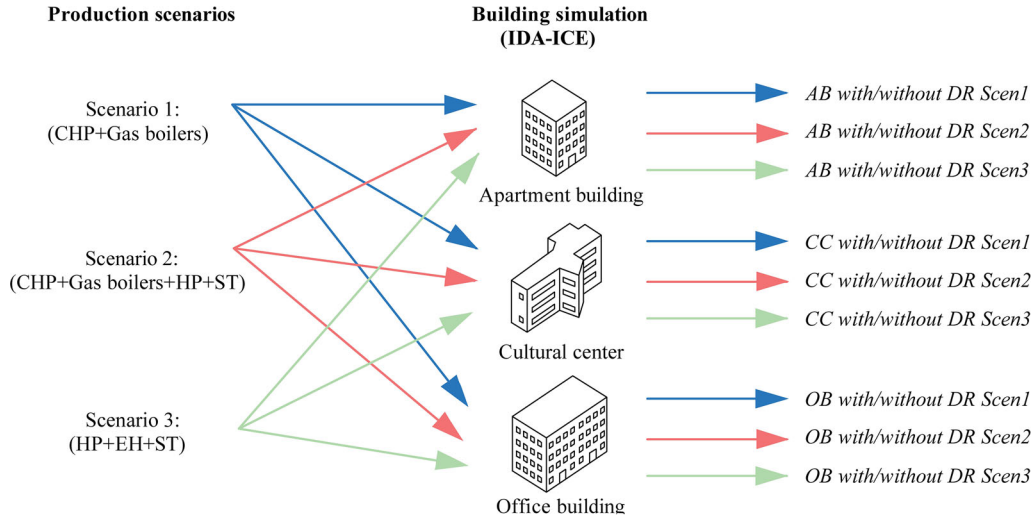
**Fig. 7.** Description of studied building cases.

$$C_{exp.} = q_{fuel} \cdot p_{fuel} + q_{el.} \cdot p_{el.} \qquad (3)$$

where $q_{fuel}$ is the fuel demand for generation, MWh; $p_{fuel}$ is the price of fuels, €/MWh; $q_{el.}$ is the consumed grid electricity for heat pump and electric heater units, MWh; and $p_{el.}$ is the market electricity price, €/MWh. The CHP unit is fed with clean bio-methane. Therefore, the DH company pays for the fuel and receives bonuses when using it. Therefore, it is possible to achieve negative costs when revenue from selling electrical energy is higher than the expenses for fuel and electricity. This situation only occurs for CHP units.

The calculation of fuel demand is shown in Eq. (4):

$$q^g_{fuel}(t) = \frac{q^g(t)}{\eta^g} \qquad (4)$$

where $g$ is the specific generation unit; $q^g_{fuel}(t)$ is the fuel demand for the generation of each unit per hour, MWh; $q^g(t)$ is the generated heat of each unit per hour, MWh; and $\eta^g$ is the generation efficiency of each unit.

The calculation of $CO_2$ emissions depends on heat generators (electricity Eq. (5)/fuel Eq. (6)):

$$m^g_{CO_2}(t) = q^g_{el.}(t) \cdot \varepsilon^g_{el.} \qquad (5)$$

$$m^g_{CO_2}(t) = q^g_{fuel}(t) \cdot \varepsilon^g_{fuel} \qquad (6)$$

where $m^g_{CO_2}(t)$ is the amount of $CO_2$ emissions per hour, tonne; $q^g_{el.}(t)$ is the consumed grid electricity for the heat pump or the electric heater per hour, MWh; $\varepsilon^g_{el.}$ is the emission factor of the consumed grid electricity for the heat pump or the electric heater, tonne/MWh; and $\varepsilon^g_{fuel}$ is the emission factor of fuels for each generator, tonne/MWh. For electricity, it was assumed that it was green electricity with the value 0 tonne/MWh in scenario 2 and it was set to 0.474 tonne/MWh in scenario 3 (Statista 2020). The value for bio-methane is 0 tonne/MWh since it counts as renewable energy. The value for gas boilers was set based on German law (BMU 2020b).

German legislation for renewable energy stipulates revenues for electricity from renewable sources fed into the grid (Blazejczak et al. 2014). The revenue is calculated differently based on the time of the permission and the type of the unit. For this study, the following method was applied due to the composition of the unit stock of the DH system. The amount of revenue was calculated as:

$$C_{rev.}(t) = q_{gen.el.}(t) \cdot \left[ p_{el.}(t) + p_{bonus} - p_{avr.el.} \right] \qquad (7)$$

where $C_{rev.}(t)$ is the revenue per hour from selling electricity by the CHP including governmental grants, €; $q_{gen.el.}(t)$ is the generated grid electricity by the CHP per hour, MWh; $p_{el.}(t)$ is the current market electricity price, €/MWh; $p_{bonus}$ is the predefined governmental bonus for selling environmentally friendly electricity, €/MWh; and $p_{avr.el.}$ is the average electricity price of the previous month, €/MWh.

The HGSO tool was applied for optimization to minimize production costs. The data on heat demand of the established community and electricity was input as hourly steps. The impact of time was considered in the optimization and all relevant heat demands, prices, costs and emissions were calculated for every hour. After that, the optimization tool HGSO minimized the following objective function of the production cost for 24 hours:

$$\min C_{prod.24h} = \min \sum_{t=1}^{24} \left[ \sum_{g \in G} C^g_{exp.}(t) - C_{rev.}(t) \right] \qquad (8)$$

where $C_{prod,24h}$ is the production cost of 24 hours, €; $G$ is the set of generation units; and $C^g_{exp.}(t)$ is the expense for each unit per hour, €; and $C_{rev.}(t)$ is the revenue per hour from selling electricity by the CHP including governmental grants, €.

Afterwards, according to the minimum production cost of 24 hours (min $C_{prod,24h}$), the production cost per hour was calculated and output by HGSO. The specific production price was defined in Eq. (9):

$$p_{prod.}(t) = \frac{C_{prod.}(t)}{Q(t)} \qquad (9)$$

where $p_{prod.}(t)$ is the specific production price per hour, €/MWh; $C_{prod.}(t)$ is the production cost per hour, €; and $Q(t)$ is the hourly heat demand of the DH network, MWh.

**Table 5.** Description of DH prices in different production scenarios.

| Scenario | Maximum (€/MWh) | Minimum (€/MWh) | Average (€/MWh) | Standard deviation (€/MWh) |
|---|---|---|---|---|
| 1 | 98.8 | 7.5 | 91.2 | 8.5 |
| 2 | 99.9 | 8.6 | 91.2 | 5.2 |
| 3 | 138.5 | 47.3 | 91.2 | 4.5 |

Heat demand was covered for every timestep by renewable heat (solar thermal energy), heat production of one or more unit(s) and stored heat as shown in Eq. (10):

$$Q(t) = \sum_{g \in G} q^g(t) + q_{storage}(t) + q_{ren.}(t) \qquad (10)$$

where $q^g(t)$ is the generated heat of each unit per hour, MWh; $q_{storage}(t)$ is charged or discharged heat per hour, MWh; and $q_{ren.}(t)$ is renewable heat generated per hour, MWh. Depending on the electricity price on the market, the HGSO tool optimized the most economical way to generate the demanded heat. It resulted in an hourly schedule operation of units and storage. Renewable heat was immediately fed into the system.

The storage can either be charged or discharged as shown below, which is described by further equations in Suhl and Mellouli's (2009) research:

$$q_{storage}(t) = q_{discharge}(t) \cdot \eta_{storage} - \frac{q_{charge}(t)}{\eta_{storage}} \qquad (11)$$

where $q_{discharge}(t)$ is discharged heat per hour, MWh; $q_{charge}(t)$ is charged heat per hour, MWh; and $\eta_{storage}$ is discharged or charged efficiency. When the heat storage is discharging, $q_{charge}$ is zero and vice versa.

Total price range ($R$) of specific production price was defined as:

$$R = \left| \min\left[ p_{prod.}(t) \right] \right| + \left| \max\left[ p_{prod.}(t) \right] \right| \qquad (12)$$

where $R$ is the total price range of specific production price in the simulated year, €/MWh.

According to the equations mentioned above, the production costs were calculated on an hourly basis considering fixed prices for gas and fuels and flexible electricity prices. On the consumer side, a new tariff structure was applied for the requirement of demand response implement, and we created an hourly DH price. Therefore, these hourly heat production costs were normalized to fit the real DH price ($p_{real}$) of 91.2 €/MWh. Therefore, the price normalization factor was defined as shown in Eq. (13) and the specific normalized DH price was calculated by Eq. (14):

$$F = \frac{p_{real}}{R} \qquad (13)$$

$$p_{DH}(t) = F \cdot \left( p_{prod.}(t) + \left| \frac{\sum_{t=1}^{8760} p_{prod.}(t)}{8760} \right| \right) + p_{real} \qquad (14)$$

where $F$ is the price normalization factor; $p_{real}$ is the real DH price, €/MWh; and $p_{DH}(t)$ is the hourly specific normalized DH price, €/MWh.

Table 5 describes DH prices in different production scenarios. The average prices are the same because of normalization. The maximum and minimum prices of scenarios 1 and 2 are quite similar. On the contrary, the DH price of scenario 1 is more fluctuated than that of scenario 2 because of a higher standard deviation. The DH price of scenario 3 has the highest maximum and minimum prices, while it is also the flattest one with the smallest standard deviation.

### Building-level rule-based demand response control

This study assumed that the moving future 24-hour price of DH was known. Control signals (CS) were calculated using the Behrang-Sirén method (Alimohammadisagvand, Jokisalo, and Sirén 2018; Vand et al. 2020). The price trend was defined as decreasing, increasing and flat with values of $-1$, $+1$ and 0. The marginal 75 €/MWh was applied in this study based on Martin's (2017) research. The control signal is formed as shown below:

$$If \begin{cases} HEP < HEP_{avr.}^{+1, +24} - marginal\ value \\ or \\ HEP_{avr.}^{+6, +12} > HEP_{avr.}^{+6, +24} + marginal\ value \end{cases}, Then\ CS = +1$$

$$Elseif \quad HEP > HEP_{avr.}^{+1, +24}, Then\ CS = -1$$

$$Else\ CS = 0$$

$$End\ If$$

$$\qquad (15)$$

where $HEP$ is the hourly district heat energy price, €/MWh; $HEP_{avr.}^{+1+24}$ is the future average DH price from hour 1 to 24, €/MWh; $HEP_{avr.}^{+6+12}$ is the future average DH price from hours 6 to 12, €/MWh; and $HEP_{avr.}^{+6+24}$ is the future average DH price from hours 6 to 24, €/MWh.

The control algorithm employed in this study is delineated in Figure 8. The main idea of the control strategy is to exploit the thermal mass of the structures as short-term energy storage by adjusting the indoor air temperature. The hourly target indoor air temperature was controlled by the space heating system. $T_{SH,\ min}$, $T_{SH,\ norm}$ and $T_{SH,\ max}$ represents the minimum indoor air temperature setpoint (20 °C), the normal indoor air temperature setpoint (21 °C), and the maximum indoor air temperature setpoint (23 °C), respectively. To avoid overheating, limiting outdoor temperature ($T_{limit,\ out}$) was chosen to be 0 °C based on Martin's (2017) research. The setpoint smoothing technique was applied for these setpoints calculated by the control algorithm (Figure 8) to minimize the rebound effect (Suhonen et al. 2020; Ju et al. 2021).
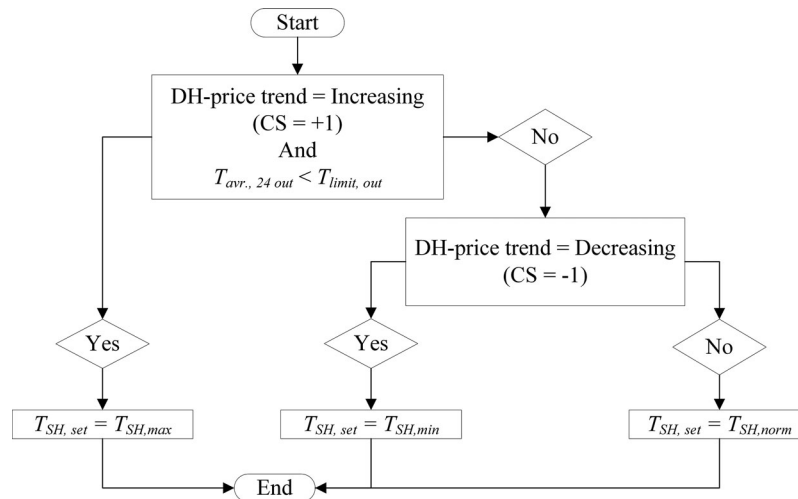
**Fig. 8.** Control algorithm for space heating.

**Table 6.** Number of total setpoint variation hours during the simulated year.

| | Temperature setpoints | | |
|---|---|---|---|
| Scenario | 20 °C | 21 °C | 23 °C |
| 1 | 5546 | 3214 | 0 |
| 2 | 5659 | 3101 | 0 |
| 3 | 2720 | 6040 | 0 |

## Results

### DR benefits for building owners

*Setpoint variations and thermal comfort*
The number of total setpoint variation hours during the whole simulated period has been summarized based on the DR control algorithm (Figure 8) with the three different DH prices as shown in Table 6. The number of hours at 20 °C is quite similar in scenarios 1 and 2, which is almost twice as many as that in scenario 3. It indicates that indoor air temperature never reached 23 °C in each scenario with the applied DR control algorithm. The main reason is that the high marginal value (75 €/MWh) decreases charging hours. The cost savings become higher as marginal value increases, while the number of charging hours decreases with higher marginal values (Alimohammadisagvand, Jokisalo, and Sirén 2018; Suhonen et al. 2020). The marginal value 75 €/MWh was chosen in this study based on Suhonen et al. (2020) to maximize the cost savings of a building owner.

The simulation results regarding the indoor air temperatures during the heating season (1 October to 31 March) of the coldest occupied rooms for the three building types with DR are presented in Figure 9. Even if there was space heating demand in October due to relatively low outdoor temperatures (the lowest was −1.4 °C), there was still a very warm week when there was no space heating demand at all because of the higher outdoor temperatures (highest was 26.9 °C). It caused the indoor air temperatures to be outside the thermal comfort range on these days. In addition, it

shows that the minimum indoor air temperatures of the coldest occupied rooms are above 20 °C all the time in the cultural center and office building, and only a maximum of 9 hours below 20 °C in the apartment building. Therefore, these simulated buildings with the DR control could maintain thermal comfort during space heating periods.

*Energy and cost savings*
Figures 10–12 show simulation results for the three building types with and without DR for three production scenarios. The total DH consumption includes heat consumption of space heating, ventilation and DHW. The differences illustrate the decrease of peak DH power, annual DH consumption and annual DH energy costs compared with the reference cases without DR in each scenario.

The objective of the rule-based demand response control is to decrease DH power during high DH price periods and reduce DH energy costs. Although the number of hours at 20 °C in scenarios 1 and 2 are almost twice as many as that of scenario 3, the differences in consumption and costs are close to each other. In addition, similar consumption and cost savings in each simulated DR case reflect that those cost savings are mainly caused by DH consumption reduction.

In the apartment building, the utilization of DR decreases a maximum of 8.4 kW peak DH power, 2.8% of consumption and 2.9% of energy costs. For the cultural center cases, DR control reduces at most 6.9 kW peak DH power. Consumption and energy cost savings are about 1% higher than those of the apartment building.

In the office building, the energy and cost savings are the highest among the three building types. The average cost-saving rate for all the office building cases is 1.9% and 0.8% higher than those of the apartment building and cultural center cases, respectively. The reason is the intermittent usage of the office building and its ventilation system. No internal heat gains during the weekends affect indoor temperatures and space heating demand. Also, the heating demand by the ventilation system is lower than other building types because the ventilation system only operated on
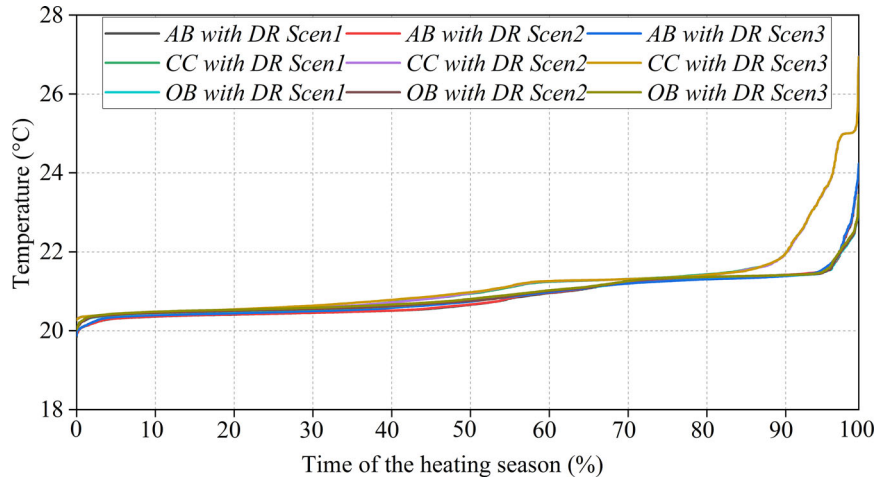
**Fig. 9.** Heating season (1 October to 31 March) duration of indoor air temperature of the coldest occupied rooms in three building types.
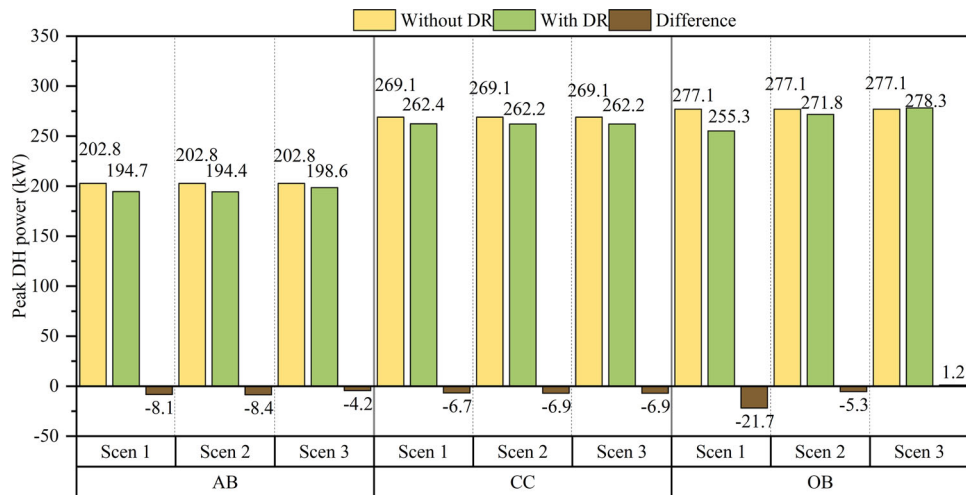


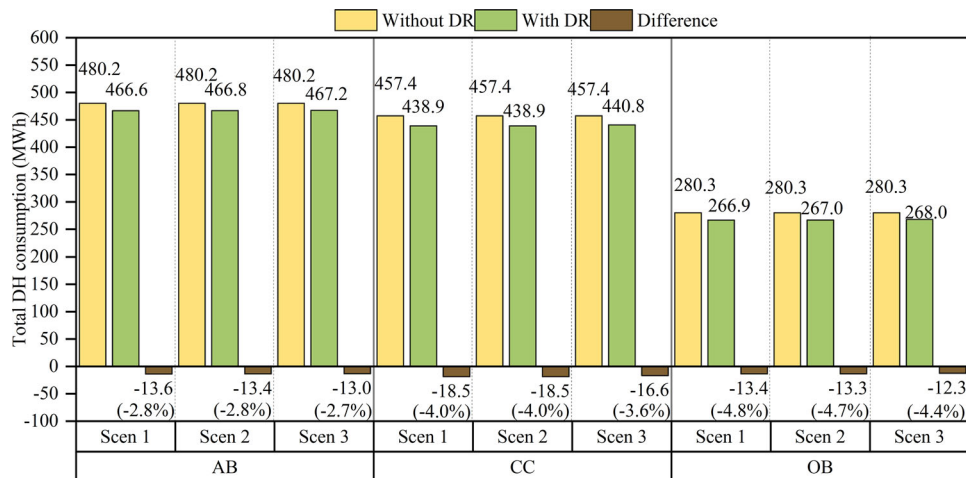**Fig. 10.** Peak DH power of three building types with and without DR in three production scenarios.



**Fig. 11.** DH consumption of three building types with and without DR in three production scenarios.
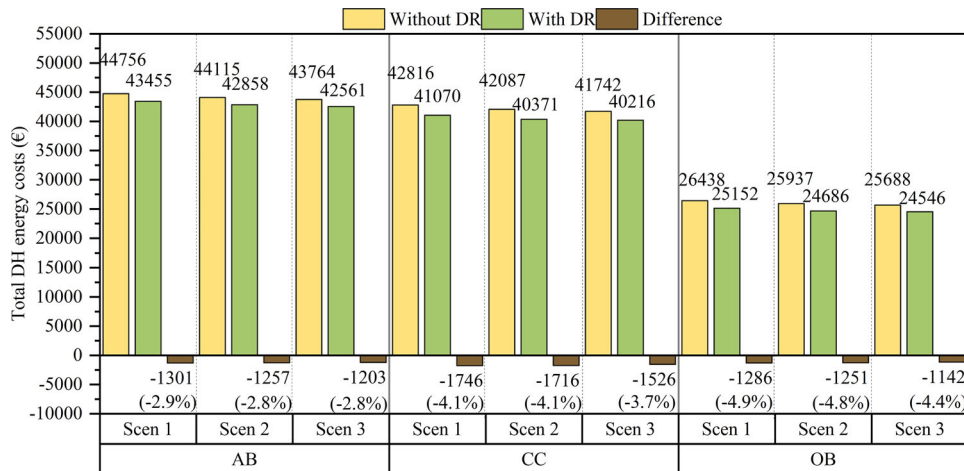
**Fig. 12.** DH energy costs of three building types with and without DR in three production scenarios.

working days. Since the DR control was only enabled on the space heating systems, the space heating consumption has more apparent changes in the office building, resulting in a more significant decrease of peak power than other building types.

### DR benefits for district heating production

#### Cost saving and $CO_2$ emission reductions

The co-simulation process explained in the beginning of methodology section and Figure 1 was executed for every scenario shown in Table 4 with and without DR control. Figure 13 shows the results, including the total DH generation of the community, $CO_2$ emissions, total energy generation costs (Eq. (2)), specific generation cost and the average generation price per MWh. The average generation price represents the average specific production price (Eq. (9)) throughout the year. The differences describe the change by DR in the examined value.

DR control decreases the total DH demand in all scenarios by 3.6%–3.9%. However, the similar demand savings result in different $CO_2$ emission reductions and total generation cost savings in each scenario.

In scenario 1, the lower DH consumption by DR leads to a cut in demand for fuels. The application of DR effectively reduces $CO_2$ emissions by 6.9%. In addition, it should be noted that it increases profits for producers by 12.6%. The overall profit per MWh increases by about 17%.

In scenario 2, since the production mix is more renewable, DR leads to the greatest reduction of $CO_2$ emissions, at 32.3%. However, the absolute $CO_2$ emission reductions are the lowest among these three scenarios. Also, producers only gain a 5.9% increase in profits by DR, which is half of the earnings in scenario 1, and the overall profit per MWh decreases by 7% compared with scenario 1.

In scenario 3, less electricity by DR is required to generate heat, resulting in lower $CO_2$ emissions. Emissions reduce by 8.6%, and DR of the total generation costs decreases by 12.3%. In addition, the DR application of the average generation price drops by 1.5%.

#### Operation of DH production units with different scenarios

Table 7 shows variations of operation hours and generated energy in three scenarios with DR during the simulated period of one year. Negative hours and energy mean that they decrease by DR. Similarly, positive values represent an increase.

In scenario 1, DR reduces operation hours for the CHP and boilers by 56 and 87 hours, respectively. The full load operation time of the CHP drops by 34 hours by DR while there is only a reduction of eight hours for the boilers. In scenario 2, the operation and full load operation hours of the CHP unit decrease close to the values for scenario 1. However, the boilers' operation hours are reduced by about twice that compared with scenario 1. The total operation time in scenario 2 sees the biggest reduction among the three scenarios. This illustrates that DR control has the most significant impact on the operation hours of units in scenario 2.

In scenario 3, DR control has no significant effect on the full load operation hours of the electric heater unit. The reduction in total generated energy is slightly lower than the values of scenarios 1 and 2. Although there is an increase in the full load operation hours of the heat pump in scenario 3, its generated heat still decreases because of lower DH demand by DR.

Therefore, the application of DR decreases the operation hours of boilers in scenarios 1 and 2, which leads to less pollution. In scenario 3, by choosing the heat pump for more full load operation hours instead of the electric heater unit, DR control contributes to a higher efficiency of production operation.

Table 8 shows energy savings and DR savings of each scenario calculated by the scaling approach, as defined in Eq. (1). It illustrates that saved costs are mainly from energy reductions in scenario 1. However, in scenarios 2 and 3, the proportion of the DR cost saving is nearly 50%. This indicates that the role of DR is more significant in energy production mixes based on the utilization of renewable energy sources. It concludes that DR has a higher relative impact on these two types of combinations, where only the peak load power capacity depends on the usage of fossil fuels.
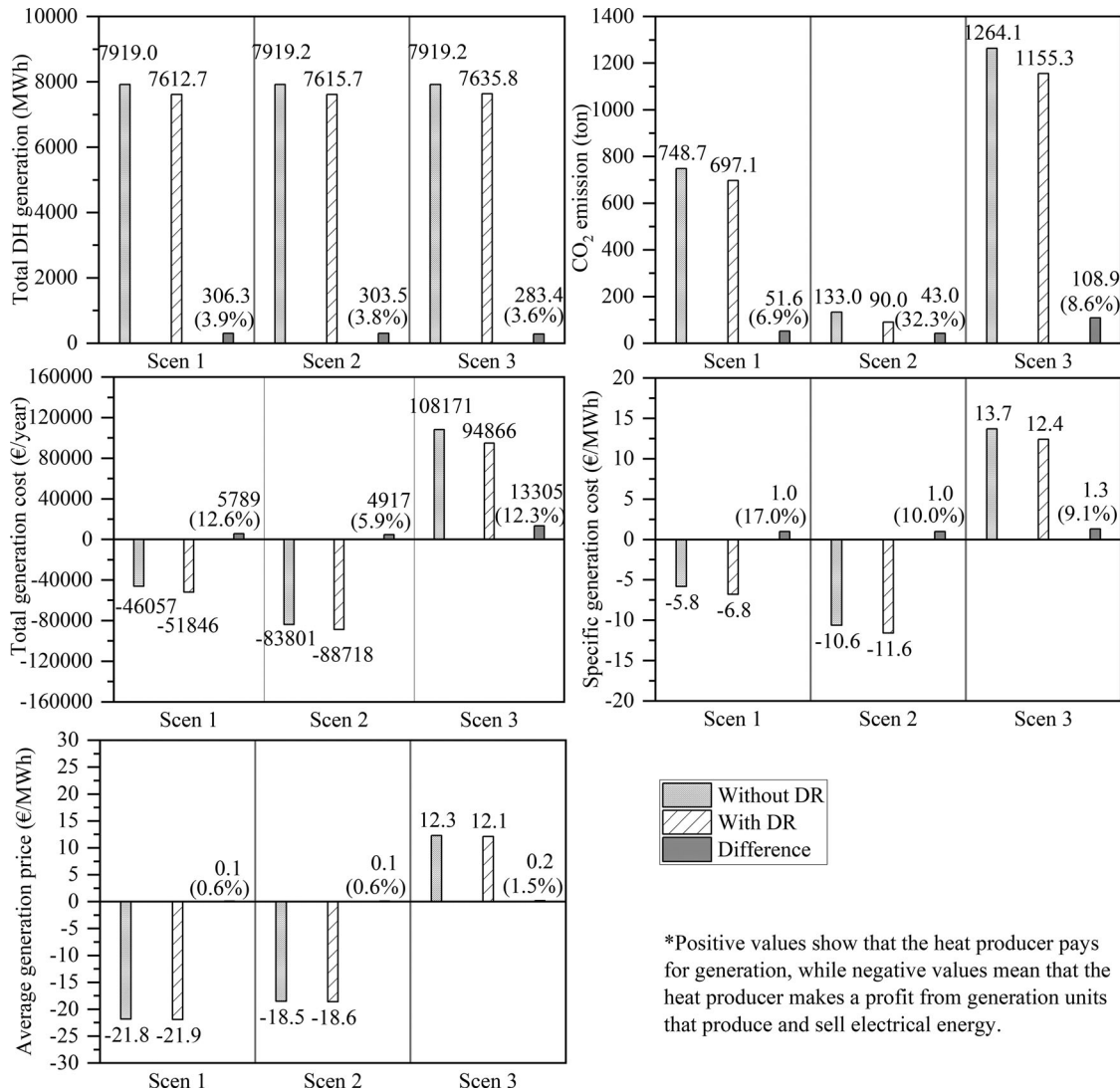
**Fig. 13.** Production scenario results with and without DR.

**Table 7.** Variations in operation hours and generated energy in three scenarios during the whole simulated period.

| Scenario | Unit | Operation hours (h) | Full load operation hours (h) | Generated energy (MWh) |
|---|---|---|---|---|
| 1 | CHP | −56 | −34 | −31.9 |
| | Boilers | −87 | −8 | −273.5 |
| | Total | −143 | −42 | −305.3 |
| 2 | CHP | −56 | −30 | −31.8 |
| | Boilers | −151 | −6 | −229.2 |
| | Heat pump | −51 | −39 | −42.7 |
| | Total | −258 | −75 | −303.6 |
| 3 | Heat pump | −29 | 55 | −87.5 |
| | Electric heater | −90 | −3 | −196.1 |
| | Total | −119 | 52 | −283.6 |

## Discussion

To realize carbon neutrality, a flexible building in a DH network is essential for increasing the proportion of renewable energies integrated into DH systems. Building-level results indicate that DR control for space heating could effectively save DH energy costs, which could be an incentive for building owners to take action toward becoming more environmentally friendly. In addition, there is motivation to increase renewable energies for commercial buildings and public buildings through social responsibility.

The large-scale application of DR could become economically and ecologically profitable for DH producers. It results

**Table 8.** Cost savings and share of DH production in three scenarios by DR.

| Scenario | Cost saving of production (€/year) | | | Cost saving share of production % | |
| --- | --- | --- | --- | --- | --- |
| | Total | Energy saving | DR saving | Energy saving | DR saving |
| 1 | 5789 | 5296 | 493 | 91.5 | 8.5 |
| 2 | 4917 | 2806 | 2111 | 57.1 | 42.9 |
| 3 | 13305 | 7138 | 6167 | 53.6 | 46.4 |

in higher financial benefits and less $CO_2$ emissions in all the analyzed scenarios. There is significantly less heat generation with the boilers, and less pollution. It indicates that large-scale application of DR could be an effective strategy to decrease fossil fuel usage, increase the proportion of renewable energy sources, and improve the energy efficiency of DH systems by increasing the operation hours of more efficient units. DH producers would pay less for $CO_2$ emissions.

With the acceleration of urbanization, the number of heating consumers is gradually increasing. This phenomenon will eventually mean that heating production systems will not be able to cover the increasing heat demand. Lower energy demand of the DH system by DR enables more connected consumers within the same generation network. DH producers may gain more profits from more consumers and save on investments in new or replacement generators.

The investment costs of power generation and building-level electronic radiator valves were not considered in this article. However, investment in electronic radiator valves for DR control could improve the controllability of DH systems, which can furthermore provide better thermal comfort and ameliorate the imbalance of water supply networks. Therefore, an investment and life cycle cost analysis should be carried out for future optimal energy production systems in further studies.

The selection of the marginal value changes the performance of the DR control algorithm. Lower marginal values are more sensitive and proactive, leading to more regular charging periods. However, the more heat is charged for in building structures, the more heat will be lost because of higher indoor air temperatures. Although higher marginal values weaken the price fluctuation effects, they could lead to higher energy and cost-saving rates than lower marginal values for building owners' values (Alimohammadisagvand, Jokisalo, and Sirén 2018; Suhonen et al. 2020). In this study, the marginal value 75 €/MWh has been applied in the DR control algorithm. Therefore, further investigations into the DR control impacts on DH production with lower marginal values should be carried out.

The control algorithm only controls space heating power demand and shifts power from high price periods to low price periods. Peak power limiting based on different usage times of buildings and DHW power demand has an impact on the peak power of the building, and the heating system could offer a further examination of the control algorithm.

Negative and positive costs for production can occur depending on the share of units in the production mix. It should be noted that DR control effects on hourly DH prices were not considered in the simulation. The hourly DH prices adopted in this study were calculated based on the hourly power demand of the DH network without DR. However, a lower energy demand of the DH system by DR results in lower production costs, which will further decrease hourly DH prices for consumers. Therefore, it should be considered whether hourly DH prices need to be adjusted when DR is applied. Moreover, the production results illustrate that a DH producer can gain more profit compared to a consumer through DR. Part of the profits should be shared fairly with consumers. Therefore, the amortization strategy of DH production benefits needs to be carried out in any further analysis and based on that, a new business models could be developed.

The building-level results are relevant to the certain building types in this study with similar climate conditions and price characteristics of studied DH production scenarios. However, the DR control algorithm employed in this study is general, which could be adopted in any building type in different climate conditions and with different prices. In addition, the production-level simulation results of energy reduction, cost saving and operation hour variation are typical of the studied DH production scenarios. In contrast, the methodology of DH production analysis is applicable for all production combinations.

The new concept, a fifth-generation district heating and cooling system, usually operates at a lower temperature with more renewable energies and industrial or urban excess heat (Buffa et al. 2019). Electrically-driven water source heat pumps for heating and cooling the supply water are integrated into a building-sited energy transfer station with TES in the system. Therefore, a DR control with TES has excellent application prospects with peak shaving, load shifting and valley filling for the grid imbalance problems and the benefits of peak demand reduction, $CO_2$ emission reduction and financial savings. However, compared with traditional DH or electricity grids, DR application in the new system should consider sector coupling of thermal and electrical grids with parameters such as supply temperatures, electricity prices, power variations, and so on.

The study considered a demand response share of 100% within the DH system. Thus, large-scale implementation of the shown demand response application requires more applied research. Today, DR measures are implemented individually with high economic investments. The challenge is to outline standardized methodologies and approaches that provide large-scale acceptance and applicability. It includes

establishing hourly (dynamic) price models for DH consumers and developing standardized communication interfaces to provide price information, to build an energy management system or cloud-based IoT electronic thermostats controllers, for example.

## Conclusions

The goal of the analysis is to identify the economic and environmental effects of the application of DR on both buildings and DH production. It was executed in the form of a co-simulation using building simulation by IDA ICE, the optimization tool HGSO for energy production, and a price signal normalization. The results showing the benefits with and without DR were analyzed from the perspectives of building owners and DH producers. The key conclusions are explained below.

From the building owners' perspective, the application of DR decreases heat energy costs. Cost-saving rates range from 2.8% to 4.9% based on different scenarios and building types. The cost-saving rate of the simulated office building cases is the highest among the three building type cases in each scenario.

From the DH producers' perspective, the large-scale application of DR decreases the total DH demand from 3.6%–3.9% and an algorithm-controlled heating strategy results in higher financial benefits and less $CO_2$ emissions in all the analyzed scenarios. The production mix in scenario 2 has a higher proportion of renewable energies than that of scenario 1 while the units in scenario 3 only consume market electricity more generated by fossil fuels. Therefore, $CO_2$ emissions in scenario 2 with the most renewable production mix are the lowest among these three scenarios, with the highest $CO_2$ emissions reduction of 32.3%. In scenarios 1 and 3, the total generation cost-saving rates are close to 13%, which are about twice that of scenario 2. In scenario 1, 91.5% of the saved costs are from energy consumption reduction. However, in scenarios 2 and 3, almost 50% of the saved costs are caused by the DR actions. Moreover, DR control increases the full load operation hours of the heat pump, leading to higher efficiency, and decreases the operation hours of the boilers, leading to less pollution. It indicates that the application of DR effectively decreases fossil fuel generation and improves the energy efficiency of DH systems.

## Nomenclature

$C_{exp.}$ = total expenses for fuel (CHP and boilers) and electricity (heat pump and electric heater units), €

$C_{exp.}^g(t)$ = expense for each unit per hour, €

$C_{prod.}$ = production costs, €

$C_{prod.}(t)$ = production cost per hour, €

$C_{prod,24h}$ = production cost over 24 hours, €

$C_{rev.}$ = revenue from selling electricity by CHP unit (including governmental grants), €

$C_{rev.}(t)$ = revenue per hour from selling electricity by CHP, including governmental grants, €

$F$ = price normalization factor

$G$ = set of generation units

$HEP$ = hourly district heat energy price, €/MWh

$HEP_{avr.}^{+1+24}$ = future average DH price from hour 1 to 24, €/MWh

$HEP_{avr.}^{+6+12}$ = future average DH price from hours 6 to 12, €/MWh

$HEP_{avr.}^{+6+24}$ = future average DH price from hours 6 to 24, €/MWh

$m_{CO_2}^g(t)$ = amount of $CO_2$ emissions per hour, tonne

$p_{avr.el.}$ = average electricity price of the previous month, €/MWh.

$p_{bonus}$ = predefined governmental bonus for selling environmentally friendly electricity, €/MWh

$p_{DH}(t)$ = hourly specific normalized DH price, €/MWh

$p_{el.}$ = market electricity price, €/MWh

$p_{el.}(t)$ = current market electricity price, €/MWh

$p_{fuel}$ = price of fuels, €/MWh

$p_{prod.}(t)$ = specific production price per hour, €/MWh

$p_{real}$ = real DH price, €/MWh

$R$ = total price range of specific production price in the simulated year, €/MWh

$q^g(t)$ = generated heat of each unit per hour, MWh

$q_{charge}(t)$ = charged heat per hour, MWh

$q_{discharge}(t)$ = discharged heat per hour, MWh

$q_{el.}$ = consumed grid electricity for heat pump and electric heater units, MWh

$Q(t)$ = hourly heat demand of the DH network, MWh.

$q_{el.}^g(t)$ = consumed grid electricity for the heat pump or the electric heater per hour, MWh

$q_{fuel}$ = fuel demand for generation, MWh

$q_{fuel}^g(t)$ = fuel demand for generation of each unit per hour, MWh

$q_{gen.el.}(t)$ = generated grid electricity by CHP per hour, MWh

$q_{ren.}(t)$ = renewable heat generated per hour

$q_{storage}(t)$ = charged or discharged heat per hour, MWh

$Q_{scaled}(t)$ = scaled hourly heat demand of the DH network, MWh

$Q_{without\ DR}(t)$ = hourly heat demand of the DH network without DR, MWh

$Q_{with\ DR}(t)$ = hourly heat demand of the DH network with DR, MWh

$t$ = the time slot with the range from 1 to 8760, h

$T_{avr.,24\ out}$ = outdoor 24 hour moving average temperature, °C

$T_{limit,\ out}$ = limiting outdoor temperature, °C

$T_{SH,\ min}$ = minimum indoor air temperature setpoint, °C

$T_{SH,\ norm}$ = normal indoor air temperature setpoint, °C

$T_{SH,\ max}$ = maximum indoor air temperature setpoint, °C

*Greek symbols*

$\eta^g$ = generation efficiency of each unit
$\eta_{storage}$ = discharged or charged efficiency
$\varepsilon_{el.}^g$ = emission factor of the consumed grid electricity
for the heat pump or the electric heater,
tonne/MWh
$\varepsilon_{fuel}^g$ = emission factor of fuels for each generator,
tonne/MWh

*Superscript*

$g$ = specific generation unit

*Subscripts*

avr. = average
el. = electricity
exp. = expense
gen. = generation
max = maximum
min = minimum
norm = normal
prod. = production
rev. = revenue
SH = space heating

*Acronyms*

AB = apartment building
CC = cultural center
CHP = combined heat and power
COP = coefficient of performance
CS = control signals
DH = district heating
DHW = domestic hot water
DR = demand response
EH = electric Heater
HEP = hourly district heat energy price
HGSO = heat generation schedule optimizer
HP = heat pump
HVAC = heating, ventilation and air conditioning
ICE = Indoor Climate and Energy
MILP = mixed-integer linear programming problem
OB = office building
TES = thermal energy storage
ST = solar thermal

## Acknowledgements

## Disclosure statement

## Funding

## ORCID

Yuchen Ju http://orcid.org/0000-0003-3432-3791
Juha Jokisalo http://orcid.org/0000-0002-7703-8838
Risto Kosonen http://orcid.org/0000-0002-9717-7552

## References

Ala-Kotila, P., T. Vainio, and J. Heinonen. 2020. Demand response in district heating market—results of the field tests in student apartment buildings. *Smart Cities* 3 (2):157–71. doi:10.3390/smartcities3020009

Alimohammadisagvand, B., J. Jokisalo, and K. Sirén. 2018. Comparison of four rule-based demand response control algorithms in an electrically and heat pump-heated residential building. *Applied Energy* 209:167–79. doi:10.1016/j.apenergy.2017.10.088

Bagherian, M. A., K. Mehranzamir, A. B. Pour, S. Rezania, E. Taghavi, H. Nabipour-Afrouzi, M. Dalvi-Esfahani, and S. M. Alizadeh. 2021. Classification and analysis of optimization techniques for integrated energy systems utilizing renewable energy sources: A review for CHP and CCHP Systems. *Processes* 9 (2):339. doi:10.3390/pr9020339

Blazejczak, J., F. G. Braun, D. Edler, and W. P. Schill. 2014. Economic effects of renewable energy expansion: A model-based analysis for Germany. *Renewable and Sustainable Energy Reviews* 40:1070–80. doi:10.1016/j.rser.2014.07.134

BMU (Federal Ministry for the Environment, Nature Conservation and Nuclear Safety). 2020a. Climate Action in Figures. Accessed September 13, 2021. https://www.bmu.de/en/publication/climate-action-in-figures-2020.

BMU (Federal Ministry for the Environment, Nature Conservation and Nuclear Safety). 2020b. Gesetz zur Einsparung von Energie und zur Nutzung erneuerbarer Energien zur Wärme-und Kälteerzeugung in Gebäuden* (Gebäudeenergiegesetz - GEG)-Anlage 9 (zu § 85 Absatz 6)-Umrechnung in Treibhausgasemissionen (Act on the Saving of Energy and the Use of Renewable Energies for Heating and Cooling in Buildings* (Building Energy Act - GEG)-Annex 9 (to § 85

paragraph 6)-Conversion into greenhouse gas emissions). Accessed September 30, 2021. https://www.gesetze-im-internet.de/geg/anlage_9.html.

Bring, A., P. Sahlin, and M. Vuolle. 1999. Models for building indoor climate and energy simulation—A report of IEA SHC Task 22: Building Energy Analysis Tools. Stockholm, IEA. Accessed April 9, 2021. https://www.equa.se/dncenter/T22Brep.pdf.

Buffa, S., M. Cozzini, M. D'antoni, M. Baratieri, and R. Fedrizzi. 2019. 5th generation district heating and cooling systems: A review of existing cases in. *Renewable and Sustainable Energy Reviews* 104:504–22. doi:10.1016/j.rser.2018.12.059

Cai, H., C. Ziras, S. You, R. Li, K. Honoré, and H. W. Bindner. 2018. Demand side management in urban district heating networks. *Applied Energy* 230:506–18. doi:10.1016/j.apenergy.2018.08.105

CEN (The European Committee for Standardization). 2007. EN 2007-13779:2007. *Ventilation for non-residential buildings–performance requirements for ventilation and room-conditioning systems*. The European Committee for Standardization. Brussels, Belgium.

Christidis, A. C. 2019. Thermische Speicher zur Optimierung des Betriebs von Heizkraftwerken in der Fernwärmeversorgung [Thermal storage for the optimisation of the operation of combined heat and power plants in district heating applications]. Doctoral thesis. Technische Universität Berlin.

De Coninck, R., and L. Helsen. 2016. Quantification of flexibility in buildings by cost curves–Methodology and application. *Applied Energy* 162:653–65. doi:10.1016/j.apenergy.2015.10.114

Dominković, D. F., P. Gianniou, M. Münster, A. Heller, and C. Rode. 2018. Utilizing thermal building mass for storage in district heating systems: Combined building level simulations and system level optimization. *Energy* 153:949–66. doi:10.1016/j.energy.2018.04.093

Equa Simulation, A. B. 2010a. *Validation of IDA Indoor Climate and Energy 4.0 with respect to CEN Standards EN 15255-2007 and EN 15265-2007*. Solna, Sweden. Accessed April 9–2021. http://www.equaonline.com/iceuser/validation/CEN_VALIDATION_EN_15255_AND_15265.

Equa Simulation, A. B. 2010b. Validation of IDA Indoor Climate and Energy 4.0 build 4 with respect to ANSI/ASHRAE Standard 140-2004. EQAU Simulation Technology Group, Sweden. Accessed April 9, 2021. http://www.equaonline.com/iceuser/validation/ASHRAE140-2004.pdf.

Euroheat & Power, and D. Moczko. 2019. District energy in Germany. Accessed April 4, 2021. https://www.euroheat.org/knowledge-hub/district-energy-germany/.

European Commission. 2018a. EU Climate Action – 2030 climate and energy framework. Accessed December 9, 2020. https://ec.europa.eu/clima/policies/strategies/2030_en.

European Commission. 2018b. Heating and cooling. Accessed December 9, 2020. https://ec.europa.eu/energy/topics/energy-efficiency/heating-and-cooling_en.

European Commission. 2020. 2050 long-term strategy. Accessed December 9, 2020. https://ec.europa.eu/clima/policies/strategies/2050_en.

European Environment Agency. 2021. Heating and cooling degree days. Accessed March 3, 2021. https://www.eea.europa.eu/data-and-maps/indicators/heating-degree-days-2.

Forrest, J., and R. Lougee-Heimer. 2005. CBC User Guide. Emerging theory, methods, and applications (pp. 257–277). INFORMS. Accessed March 4, 2021. https://pubsonline.informs.org/doi/10.1287/educ.1053.0020.

Freja, E. 2020. Heating 40 million homes – the hurdles to phasing out fossil fuels in German basements. Clean Energy Wire (CLEW). Accessed December 16, 2020. https://www.cleanenergywire.org/factsheets/heating-40-million-homes-hurdles-phasing-out-fossil-fuels-german-basements.

Gelazanskas, L., and K. A. Gamage. 2014. Demand side management in smart grid: A review and proposals for future direction. *Sustainable Cities and Society* 11:22–30. doi:10.1016/j.scs.2013.11.001

Hedegaard, R. E., M. H. Kristensen, T. H. Pedersen, A. Brun, and S. Petersen. 2019. Bottom-up modelling methodology for urban-scale analysis of residential space heating demand response. *Applied Energy* 242:181–204. doi:10.1016/j.apenergy.2019.03.063

Henriksson, J., and S. Rudén. 2018. Investigation of the Improvement Potential of Heat Load Forecasts in BoFiT. Master's Thesis., Royal Institute of Technology.

Hu, M., and F. Xiao. 2018. Price-responsive model-based optimal demand response control of inverter air conditioners using genetic algorithm. *Applied Energy* 219:151–64. doi:10.1016/j.apenergy.2018.03.036

Jensen, S. Ø., A. Marszal-Pomianowska, R. Lollini, W. Pasut, A. Knotzer, P. Engelmann, A. Stafford, and G. Reynders. 2017. IEA EBC annex 67 energy flexible buildings. *Energy and Buildings* 155:25–34. doi:10.1016/j.enbuild.2017.08.044

Johra, H., P. Heiselberg, and J. Le Dréau. 2019. Influence of envelope, structural thermal mass and indoor content on the building heating energy flexibility. *Energy and Buildings* 183:325–39. doi:10.1016/j.enbuild.2018.11.012

Ju, Y., J. Jokisalo, R. Kosonen, V. Kauppi, and P. Janßen. 2021. Analyzing power and energy flexibilities by demand response in district heated buildings in Finland and Germany. *Science and Technology for the Built Environment* 27 (10):1440–60. doi:10.1080/23744731.2021.1950434

Junker, R. G., A. G. Azar, R. A. Lopes, K. B. Lindberg, G. Reynders, R. Relan, and H. Madsen. 2018. Characterizing the energy flexibility of buildings and districts. *Applied Energy* 225:175–82. doi:10.1016/j.apenergy.2018.05.037

Knudsen, M. D., and S. Petersen. 2016. Demand response potential of model predictive control of space heating based on price and carbon dioxide intensity signals. *Energy and Buildings* 125:196–204. doi:10.1016/j.enbuild.2016.04.053

Knudsen, M. D., and S. Petersen. 2017. Model predictive control for demand response of domestic hot water preparation in ultra-low temperature district heating systems. *Energy and Buildings* 146:55–64. doi:10.1016/j.enbuild.2017.04.023

Kontu, K., J. Vimpari, P. Penttinen, and S. Junnila. 2018. City scale demand side management in three different-sized district heating systems. *Energies* 11 (12):3370. doi:10.3390/en11123370

Kozarcanin, S., G. B. Andresen, and I. Staffell. 2019. Estimating country-specific space heating threshold temperatures from national gas and electricity consumption data. *Energy and Buildings* 199:368–80. doi:10.1016/j.enbuild.2019.07.013

Le Dréau, J., and P. Heiselberg. 2016. Energy flexibility of residential buildings using short term heat storage in the thermal mass. *Energy* 111:991–1002. doi:10.1016/j.energy.2016.05.076

Loga, T., and U. Imkeller-Benjes. 1997. Energiepass Heizung/Warmwasser [Energy demand heating/hot water]. Institut Wohnen und Umwelt (IWU). Darmstadt. Accessed March 5, 2021. https://www.iwu.de/fileadmin/tools/ephw/1997_IWU_LogaImkeller-Benjes_Energiepass-Heizung-Warmwasser-EPHW.pdf.

Lu, Z., and L. Shumei. 2018. The Status Analysis and Development Outlook of the Regional Multi-Energy System (RMES). In 2018 IEEE 2nd International Electrical and Energy Conference (CIEEC) (pp. 687–692). IEEE. doi:10.1109/CIEEC.2018.8745736

Martin, K. 2017. Demand response of heating and ventilation within educational office buildings. Master's Thesis., Aalto University.

Merkert, L., and P. M. Castro. 2020. Optimal scheduling of a district heat system with a combined heat and power plant considering pipeline dynamics. *Industrial & Engineering Chemistry Research* 59 (13):5969–84. doi:10.1021/acs.iecr.9b06971

Merkert, L., A. A. Haime, and S. Hohmann. 2019. Optimal scheduling of combined heat and power generation units using the thermal inertia of the connected district heating grid as energy storage. *Energies* 12 (2):266. doi:10.3390/en12020266

Mikola, A., T. Kalamees, and T. A. Kõiv. 2017. Performance of ventilation in Estonian apartment buildings. *Energy Procedia.* 132:963–8. doi:10.1016/j.egypro.2017.09.681

Miller, W., and M. Senadeera. 2017. Social transition from energy consumers to prosumers: Rethinking the purpose and functionality of eco-feedback technologies. *Sustainable Cities and Society* 35: 615–25. doi:10.1016/j.scs.2017.09.009

Moosberger, S. 2007. IDA ICE CIBSE-validation: Test of IDA indoor climate and energy version 4.0 according to CIBSE TM33, issue 3. EQAU Simulation Technology Group, Sweden. Accessed April 9, 2021. http://www.equaonline.com/iceuser/validation/ICE-Validation-CIBSE_TM33.pdf.

Nuytten, T., B. Claessens, K. Paredis, J. Van Bael, and D. Six. 2013. Flexibility of a combined heat and power system with thermal energy storage for district heating. *Applied Energy* 104:583–91. doi:10.1016/j.apenergy.2012.11.029

ProCom GmbH. 2020a. BoFiT optimization. Accessed December 7, 2020. https://procom-energy.de/en/products/bofit-optimization/.

ProCom GmbH. 2020b. BoFiT. Accessed December 7, 2020. https://procom-energy.de/en/tag/bofit/.

Revesz, A., P. Jones, C. Dunham, G. Davies, C. Marques, R. Matabuena, J. Scott, and G. Maidment. 2020. Developing novel 5th generation district energy networks. *Energy* 201:117389. doi:10.1016/j.energy.2020.117389

Reynders, G., J. Diriken, and D. Saelens. 2017. Generic characterization method for energy flexibility: Applied to structural thermal storage in residential buildings. *Applied Energy* 198:192–202. doi:10.1016/j.apenergy.2017.04.061

Robert, F. C., G. S. Sisodia, and S. Gopalan. 2018. A critical review on the utilization of storage and demand response for the implementation of renewable energy microgrids. *Sustainable Cities and Society* 40:735–45. doi:10.1016/j.scs.2018.04.008

Sahlin, P. 1996. *Modelling and simulation methods for modular continuous systems in buildings*. Stockholm, Sweden: Royal Institute of Technology.

Salo, S., A. Hast, J. Jokisalo, R. Kosonen, S. Syri, J. Hirvonen, and K. Martin. 2019. The impact of optimal demand response control and thermal energy storage on a district heating system. *Energies* 12 (9):1678. doi:10.3390/en12091678

Sameti, M., and F. Haghighat. 2017. Optimization approaches in district heating and cooling thermal network. *Energy and Buildings* 140:121–30. doi:10.1016/j.enbuild.2017.01.062

Seppänen, O., N. Brelih, G. Goeders, and A. Litiu. 2012. Health based ventilation guidelines for Europe. Work package 5. Existing buildings, building codes, ventilation standards and ventilation in Europe. The Final Report. REHVA. Brussels. Accessed March 5, 2021. https://webgate.ec.europa.eu/chafea_pdb/assets/files/pdb/20091208/20091208_d05_oth5_en_ps.pdf.

SFS-EN 16798-1. 2019. *Energy performance of buildings. Ventilation for buildings. Part 1: Indoor environmental input parameters for design and assessment of energy performance of buildings addressing indoor air quality, thermal environment, lighting and acoustics. Module M1-6.* Finnish Standards Association (SFS). Helsinki.

Shan, K., S. Wang, C. Yan, and F. Xiao. 2016. Building demand response and control methods for smart grids: A review. *Science and Technology for the Built Environment* 22 (6):692–704. doi:10.1080/23744731.2016.1192878

Song, M., K. Alvehag, J. Widén, and A. Parisio. 2014. Estimating the impacts of demand response by simulating household behaviours under price and $CO_2$ signals. *Electric Power Systems Research* 111:103–14. doi:10.1016/j.epsr.2014.02.016

Statista. 2020. Entwicklung des CO2-Emissionsfaktors für den Strommix in Deutschland in den Jahren 1990 bis 2020 (Development of the CO2 emission factor for the electricity mix in Germany in the years 1990 to 2020). Accessed September 29, 2021. https://de.statista.com/statistik/daten/studie/38897/umfrage/co2-emissionsfaktor-fuer-den-strommix-in-deutschland-seit-1990/.

Stinner, S.,. K. Huchtemann, and D. Müller. 2016. Quantifying the operational flexibility of building energy systems with thermal energy storages. *Applied Energy* 181:140–54. doi:10.1016/j.apenergy.2016.08.055

Suhl, L., and T. Mellouli. 2009. *Optimierungssysteme: Modelle, Verfahren, Software, Anwendungen [Optimization systems: models, processes, software, applications]*. Berlin, Heidelberg: Springer Gabler, 100ff.

Suhonen, J., J. Jokisalo, R. Kosonen, V. Kauppi, Y. Ju, and P. Janßen. 2020. Demand response control of space heating in three different building types in Finland and Germany. *Energies* 13 (23):6296. doi:10.3390/en13236296

Tereshchenko, T., and N. Nord. 2016. Energy planning of district heating for future building stock based on renewable energies and increasing supply flexibility. *Energy* 112:1227–44. doi:10.1016/j.energy.2016.04.114

Tillmann, P. 2017. Entwicklung einer Einsatzoptimierung von Wärmeerzeugern zur wirtschaftlichen Bewertung unterschiedlicher Integrationskonzepte tiefer Geothermie in einem Nahwärmenetz [Development of an optimization for the use of heat generation units for the economic evaluation of different integration concepts of deep geothermal energy in a local heating network]. Master's Thesis. Hamburg University of Applied Sciences. Unpublished.

Vand, B., K. Martin, J. Jokisalo, R. Kosonen, and A. Hast. 2020. Demand response potential of district heating and ventilation in an educational office building. *Science and Technology for the Built Environment* 26 (3):304–19. doi:10.1080/23744731.2019.1693207

Vattenfall Wärme, H. and Hamburg GmbH. 2019. Preisblatt 2. Quartal 2019. (Price sheet 2nd Quarter 2019). Accessed March 7, 2020. https://waerme.hamburg/media/71/download/Preisblatt_Hamburg_Q2-2019.pdf?v=2.

Vogt, M., F. Marten, and M. Braun. 2018. A survey and statistical analysis of smart grid co-simulations. *Applied Energy* 222:67–78. doi:10.1016/j.apenergy.2018.03.123

Werner, S. 2017. International review of district heating and cooling. *Energy* 137:617–31. doi:10.1016/j.energy.2017.04.045

Wu, Y., A. Mäki, J. Jokisalo, R. Kosonen, S. Kilpeläinen, S. Salo, H. Liu, and B. Li. 2021. Demand response of district heating using model predictive control to prevent the draught risk of cold window in an office building. *Journal of Building Engineering* 33: 101855. doi:10.1016/j.jobe.2020.101855

Zafar, R., A. Mahmood, S. Razzaq, W. Ali, U. Naeem, and K. Shehzad. 2018. Prosumer based energy management and sharing in smart grid. *Renewable and Sustainable Energy Reviews* 82: 1675–84. doi:10.1016/j.rser.2017.07.018